

## **Full-Scale Field Compression Load Test Performed on ACIP Pile in Sand for Bridge Support**

**K. Vembu, V. Gattu and C. Vipulanandan, Ph.D., P.E.**

Center for Innovative Grouting Materials and Technology (CIGMAT)  
University of Houston, Houston, Texas 77204-4003.

Email: [CVipulanandan@uh.edu](mailto:CVipulanandan@uh.edu)

### **ABSTRACT**

In this study the performance of a non-displacement auger cast-in-place (ACIP) pile in sand under compression loading was investigated by performing a field load test. In this full-scale load test study ACIP piles were installed in layered sand, with loose sand (minimum Texas cone penetrometer (TCP) blow count of 7) in the top 4 m with very dense sand (maximum TCP blow count of 95) in the bottom layer 7 m below ground. The load test was performed on a 760 mm (30 inch) diameter fully instrumented ACIP pile with eight 450 mm (18 inch) diameter reaction piles. The test pile utilized a load cell and multiple pile top dial gages to measure applied load and settlement during the load test. Also, vibrating-wire sister bar strain gages with thermocouples were attached along the length of the test pile and selected reaction piles. The design load for the test pile was 816 kN (92 tons) and the test pile was loaded to 2840 kN (320 tons) before unloading. Using the Vipulanandan ACIP pile model the ultimate capacity was predicted to be 4545 kN (512 tons), more than five times the design capacity. Skin friction-displacement relationships for the test pile in compression and reaction piles in tension were developed with depth representing the loose to very dense sand. The maximum skin friction measured in the very dense sand was 210 kPa (2.2 tsf) in compression and 57.3 kPa (0.6 tsf) in tension. The measured skin friction in the ACIP test pile in compression was more than 50% higher than the TxDOT design standard for drilled shafts in high blow count dense sands.

### **INTRODUCTION**

ACIP piles are increasingly used for supporting building, bridges, sound barrier walls and many other structures around the world (Neely, 1991; O'Neill, 1994; Brettmann et al. 2005; Brown 2005; Vipulanandan et al. 2005- 2012). These piles have been used in the private sector in the United States for over 50 years (O'Neill et al. 1999) and became very popular in the early 1990s because of the developments in the construction quality control systems. Fast installation, high capacity, low cost and no vibrations are some reasons for the tremendous growth in ACIP pile usage. ACIP piles can be distinguished from drilled shafts and driven piles by the magnitude of effective stress changes they produce in the surrounding soil during the construction (O'Neill, 1994). Therefore, considering the principle of effective stress, the load-displacement behavior of the ACIP pile falls in between that of a drilled shaft and a driven pile (O'Neill, 1999, Vipulanandan 2005).

Load-displacement measured at the pile head provides the capacity of the pile but gives no information on the load transfer mechanism which is split between the shaft resistance distribution and toe resistance. This information is needed in order to design a safe and economical pile.

Therefore, conventional pile load tests are being instrumented more frequently to provide the load transfer along the pile (Fellenius, 2001, Vipulanandan et al. 2009 and 2012).

## **OBJECTIVES**

The overall objective of this study was to investigate the load transfer mechanism of ACIP piles under compressive and tensile loading in sand. Specific objectives are as follows:

- 1) Compare the load transfer mechanism and load-displacement relationships in layered sand for a 760 mm (30 inch) diameter ACIP pile in compression and 450 mm (18 inch) reaction ACIP piles in tension.
- 2) Model the skin friction-displacement relationships in different layers of sand for the pile in compression and reaction piles in tension.

## **FULL-SCALE FIELD TEST**

In order to better characterize the behavior of ACIP piles under axial loading, a full scale load test on instrumented ACIP piles was performed next to SH-7 near Lufkin, Texas to demonstrate the load carrying capacity to support a highway bridge over the East Cochino Bayou (ECB). The site was located in the Crockett formation which is an Eocene-aged deposit under Clairborne group. The bridge site consisted of sandy soil profiles from loose to very dense sand. Figure 1 shows the instrumentation and geotechnical profile at the ECB test site. The top layer with loose sand was up to a depth of 4 m (13 ft) with a 3 m (10 ft) thick dense sand layer 7 m below ground. Test pile was 10 m (33.1 ft) long and almost 3 m (10 ft) of the pile was socketed into the dense sand layer.

### **(a) Construction of Test Piles**

One of the main concerns when using ACIP piles is the possibility of decompression of soil surrounding the pile during drilling. Control of the rate of auger penetration will avoid decompression of the ground, loosening of the in-situ soil, and ground subsidence (Brown, 2005). If the velocity of the auger penetration is less than the critical velocity (Viggiani, 1989), decompression will occur. The critical rate of penetration of the auger for the test pile was found to be 30 mm/sec (1.2 in/sec). A grout ratio of 1.15 times the theoretical volume (DFI 2016) was satisfied at every depth interval for the test pile. Maximum grout pressure was held almost constant and was around 1380 kN/m<sup>2</sup> (200 psi).

In this study, the reinforcing cage for the pile was instrumented with vibrating wire (VW) sister bar strain gages (Fig. 1) which are essentially strain gauges that operate on the vibrating wire principle rather than the electric resistance principle common to most strain gauges (McRae and Simmonds, 1991). The gauges provide values of strain ( $\epsilon$ ) which was multiplied by the cross sectional area ( $A = 0.46 \text{ m}^2$ ;  $707 \text{ in}^2$ ) and the elastic modulus of the pile ( $E = 28 \text{ GPa}$ ;  $4 \times 10^6 \text{ psi}$ ) to find the transferred load at each level ( $\epsilon EA$ ) (Vipulanandan et al. 2009, 2012). The instrumented reaction piles with the schematic of the loading frame set up is shown in Fig. 2.

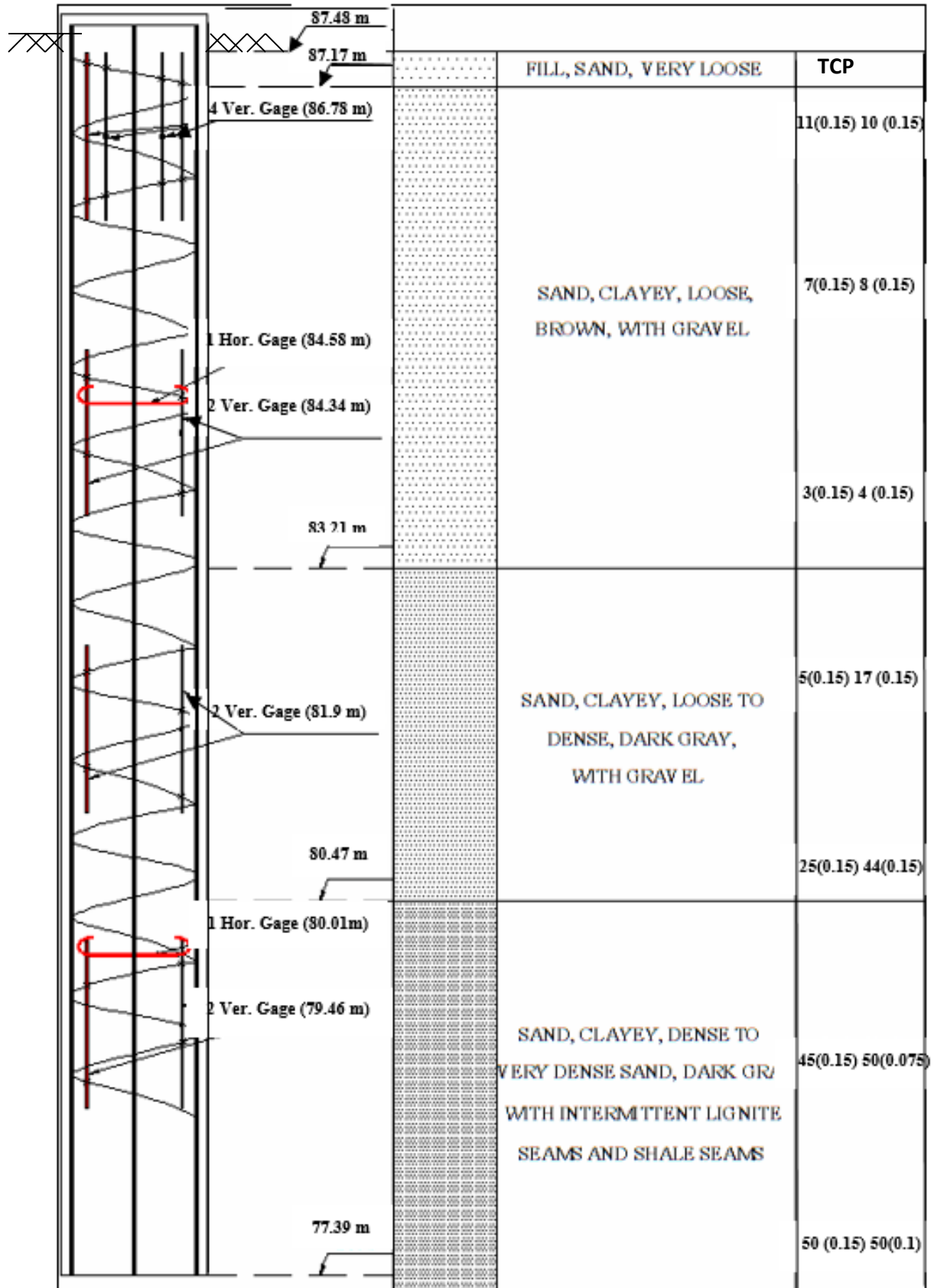
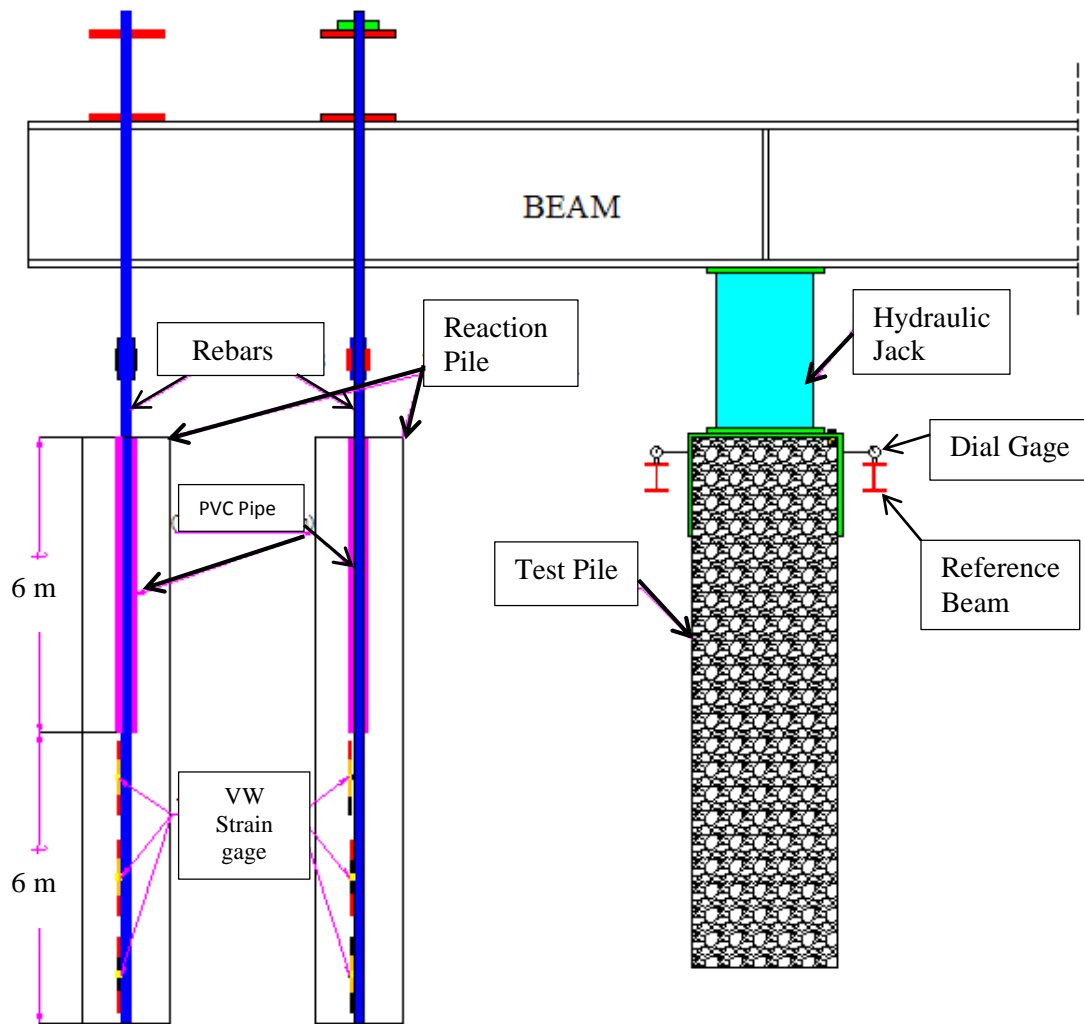


Figure 1 Instrumentation and Geotechnical Profile at ECB Site



**Figure 2. Instrumentation of the Reaction Piles and Schematic of the Load Test Configuration**

The reinforcement was debonded from grout in the top 6 m (20 ft) to avoid the cracking in the grout due to the pull-out load on the reinforcement.

### (b) Full-Scale Load Tests

The full-scale axial load test was performed using the ASTM D1143, “Standard Method of Testing Piles under Static Axial Compression load. Load was applied to the piles using a hydraulic jack acting against an anchored reaction beam. Eight reaction piles (450 mm in diameter and 13 m (40 feet) long) spaced 3 m (10 ft.) from each other (4 on each side of the test pile) and 6 m (20 ft.) from the test pile were used to provide the adequate reaction capacity. A calibrated load cell and multiple dial gages were used to measure applied load and settlement during the load test.

The pile was loaded in 90 kN (10 tons) increments up to 1775 kN (200 tons) and the increments were then increased to 180 kN (20 tons) up to 2840 kN (320 tons). The deflection at the pile design load of 816 kN (92 tons) was 1 mm. The maximum deflection measured was 9.14 mm (0.36 in.) at final load of 2840 kN (320 tons) and there was a residual displacement of 4.5 mm

(0.18 in.) after unloading. The load–displacement measurements for the ACIP test pile is shown in Fig. 3. The pile was unloaded in four equal decrements.

**Modeling**

Based on the observed trend the Vipulanandan load (Q) –displacement (ρ) ACIP pile model (Vipulanandan et al. 2005) was used to predict the behavior.

$$\frac{Q}{Q_{ult}} = \frac{(\frac{\rho}{d})}{(\frac{\rho}{d}) + (\frac{\rho_{50}}{d})} \tag{1}$$

Where Q is the load and Q<sub>ult</sub> is the ultimate load at very large settlement. The settlement is represented as ρ and ρ<sub>50</sub> is the settlement at 50% of the ultimate load. Using Eqn. (1), with two unknowns (Q<sub>ult</sub> and ρ<sub>50</sub>), nonlinear least square method (NLSM) (maximum R<sup>2</sup> and minimum RMSE) was used with 27 data to determine the two unknowns. The ultimate capacity (Q<sub>ult</sub>) of the pile was determined to be 4545 kN (512 tons). The ρ<sub>50</sub> was 5.49 mm (at half (50%) of the ultimate pile capacity of 2272 kN (256 tons)). The coefficient of variation (R<sup>2</sup>) and root mean square error of the prediction model was 0.99 and 72.06 kN respectively. Hence the pile was loaded to 62.5% of the ultimate capacity.

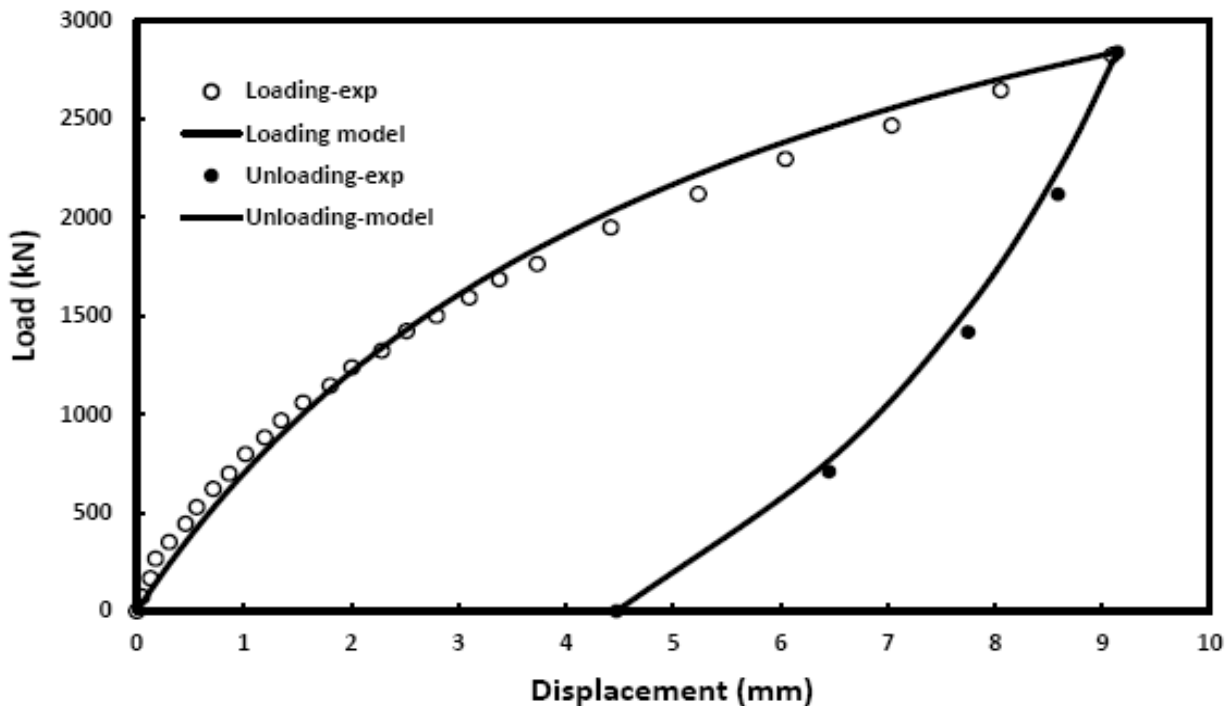


**Figure 3. Measured and Predicted Load-Displacement Relationship for the ACIP Test Pile**

The unloading relationship was represented as follows:

$$\frac{Q}{Q_*} = \frac{(\frac{\rho - \rho_0}{\rho_* - \rho_0})}{\alpha - \beta(\frac{\rho - \rho_0}{\rho_* - \rho_0})} \tag{2}$$

Where  $Q$  is the load,  $Q^*$  is the peak load at the peak load and  $\rho^*$  is the corresponding displacement at the peak load. The residual displacement  $\rho_0$  was 4.5 mm. Based on nonlinear least square method (NLSM) with 5 data the two model parameters  $\alpha$  and  $\beta$  were determined to be 2 and 1 respectively. The coefficient of variation ( $R^2$ ) and root mean square error of the prediction model was 0.99 and 79.39 kN respectively.

**Load Transfer Behavior**

The load distribution along the length of the test pile and reaction piles were calculated from the strain measured from the sister bars. Strain values were measured using the vibrating wire gages at four levels along the test pile and three levels along the reaction piles. The applied load at the top of the pile was measured using a load cell. Axial rigidity was assumed to be constant all along the length of the test pile. Load on the reaction pile was determined by measuring the strain in the reinforcing bar. The load distribution curves for the test pile and a typical reaction pile are shown in Fig. 4 and Fig. 5, respectively. The load distribution curve at the maximum load 2840 kN (320 tons) showed that the 360 kN (40.5 tons) load was carried at the tip of the pile, which was about 13% of the total applied load. For the reaction pile the maximum load at the top was 400 kN (45 tons) while the load carried near the tip of the reaction pile (skin friction) was 49 kN (5.5 tons), which was 12% of the total load.

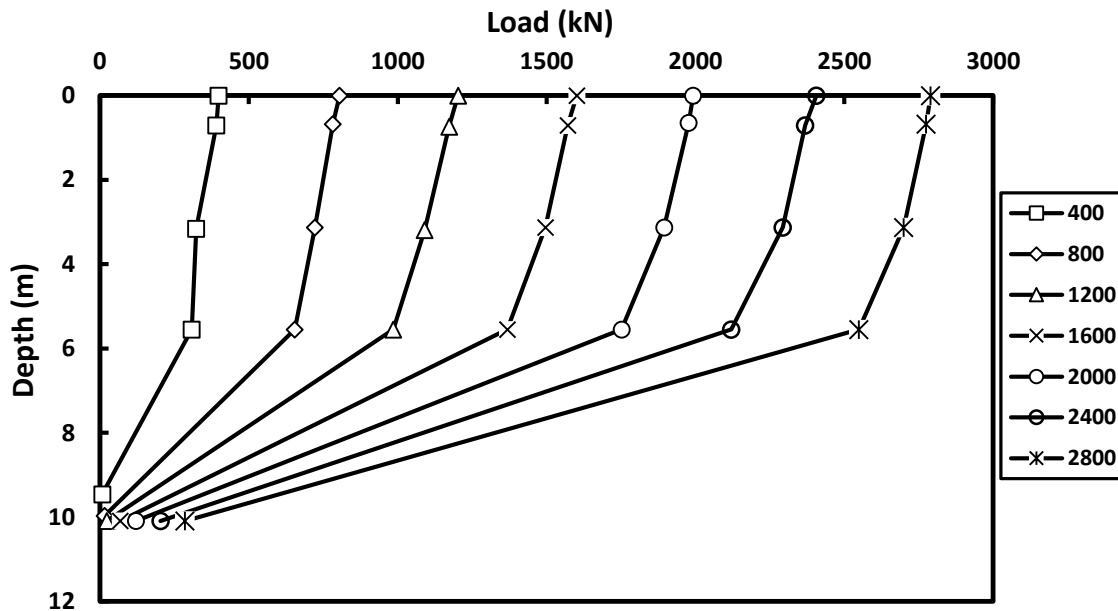


Figure 4. Load distribution along the Test Pile

**Side Skin Friction –Displacement Relationships**

**Test Pile (TP)**

The unit load transfer curves at selected depths along the pile were calculated from the slope of the linearly connected lines from the load distribution curves (Fig. 4). Each of the resulting values was divided by the nominal circumference of the pile to give unit side friction. Based on the instrumentation and measurements, the pile analyses were divided into a top segment (TP Seg-1) from 0- 3.13 m (0 – 10.3 ft.), middle segment (TP Seg-2) from 3.14 to 5.58 m (10.3 to 18.3 ft.)

and the bottom segment from 5.58 to 8 m (18.3 ft to 26.24 ft). The maximum measured side friction for dense sand in the test pile was 210 kPa (2.2 tsf), which was about four times greater than maximum skin friction developed in the reaction piles.

**TP Segment-1:** The side friction-displacement relationships for the top segment from 0- 3.13 m (0-10.3 ft) is shown in Fig. 6a was 11.5 kPa (0.12 tsf) at 8.9 mm (0.35 in.) displacements respectively. Based on the proposed model (Eqn. (3), Vipulanandan (2005-2016)) the ultimate skin friction will be 11.9 kPa (0.12 tsf). The average TCP blow count was 11 (average of 15 and 7) and the TxDOT design drilled shaft skin friction is 18.5 kPa (TxDOT Geotechnical Manual). Hence the measured skin friction was 6.6 kPa (0.07 tsf) lower than the skin friction for the drilled shaft.

**TP Segment-2:** The side friction-displacement relationship for the mid segment from 3.14 to 5.58 m (10.3-18.3 ft) shown in Fig. 6a was 22.9 kPa (0.24 tsf) at 8.4 mm (0.33 in.) displacement. Based on the proposed model (Eqn. (3)) the ultimate skin friction will be 25 kPa. The average TCP blow count was 14.5 (average of 7 and 22) the TxDOT design drilled shaft skin friction is 24.4 kPa (0.25 tsf) (TxDOT Geotechnical Manual). Hence the measured skin friction was the same as the skin friction for the drilled shaft.

**TP Segment-3:** The side friction-displacement relationships for the bottom segment to be 5.58 to 8 m (18.3 ft to 26.24 ft) shown in Fig. 6b was 210 kPa (2.2 tsf) at 7.6 mm (0.30 in.) displacement. Based on the proposed skin friction- displacement model (Eqn. (3)) the ultimate skin friction will be 303 kPa (3.2 tsf).

$$f_{sc} = \frac{s/D}{A+B\left(\frac{s}{D}\right)} \tag{3}$$

$$f_{sc}^u = \frac{1}{B}$$

The model parameters A and B were determined using the NLSM and are summarized in Table 1 with the coefficient of variation ( $R^2$ ) and root mean square error of the prediction model.

**Table 1. Model Parameters for Skin Friction-Displacement Relationships**  
**Table 1. Model Parameters for Skin Friction-Displacement Relationships**

| Test Piles   | A (kPa <sup>-1</sup> ) | B (kPa <sup>-1</sup> ) | R <sup>2</sup> | RMSE (kPa) |
|--------------|------------------------|------------------------|----------------|------------|
| Segment-TP1  | 3.50 E-05              | 0.084                  | 0.96           | 0.67       |
| Segment -TP2 | 4.50 E-05              | 0.040                  | 0.97           | 1.08       |
| Segment-TP3  | 2.0 E-05               | 0.0033                 | 0.98           | 8.14       |

**TCP Correlation**

Based on this pile load test the TCP blow count (N) was related to the maximum measured skin friction in compression for the ACIP pile as follows:

$$(f_{sc})_{\text{max. measured}} \text{ (kPa)} = 2.8 N - 18.3 \quad (N \geq 7) \tag{4}$$

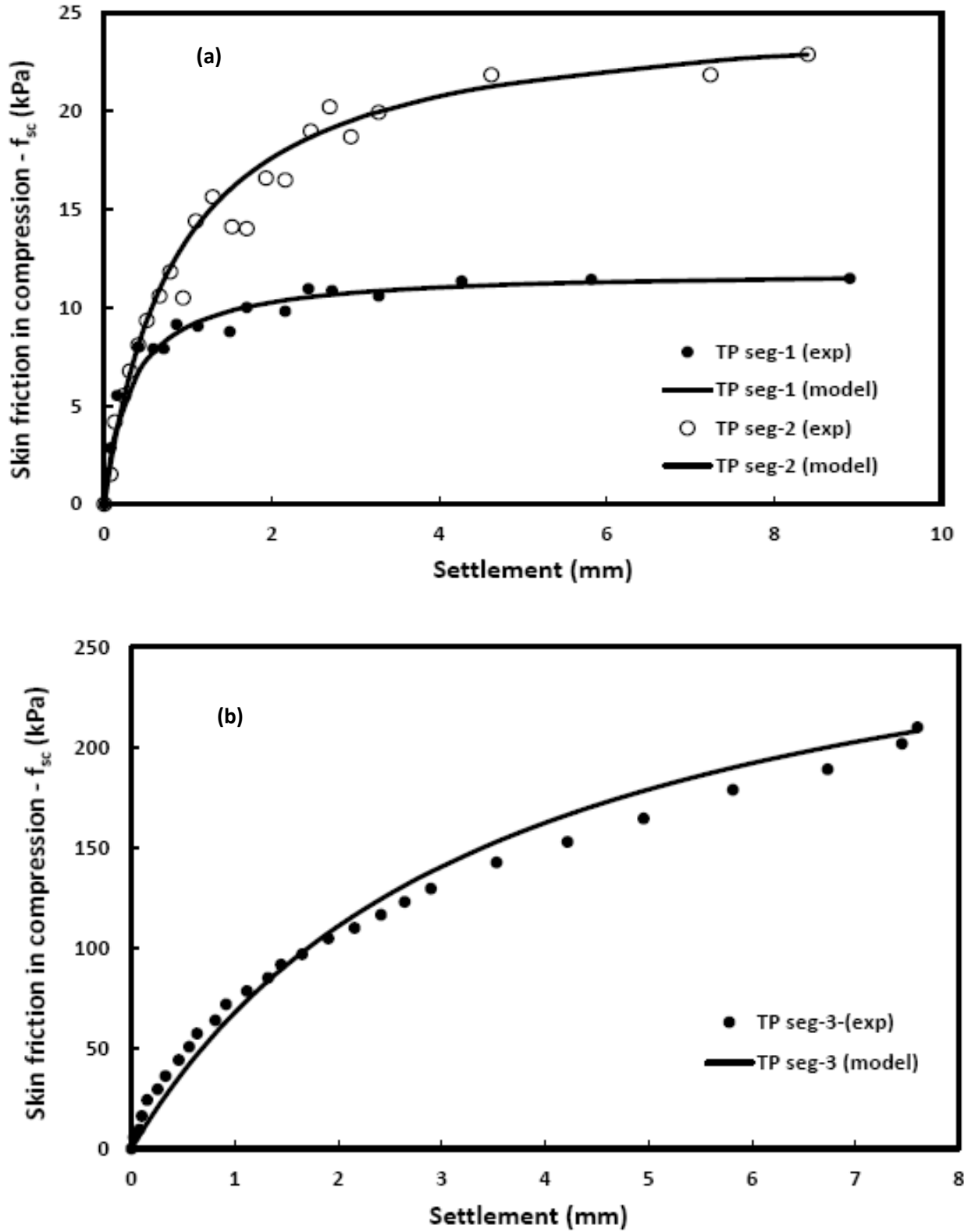


Figure 6. Measured and Modelled Skin friction (Compression)-displacement Relationship for Segments.

The TxDOT correlation for drilled shaft allowable skin friction in compression is 1.7N (reduction factor of 0.7 was applied) (TxDOT Geotechnical Manual). The relationships are compared in Fig. 7. When the average TCP blow count was 82 (average of 69 and 95) around 8 m (24 ft) below ground the TxDOT design drilled shaft skin friction allowed is 137.8 kPa (1.4 tsf). Hence the measured ACIP skin friction was 210 kPa (2.2 tsf), which was over 50% higher than the allowable skin friction for the drilled shaft.

## CONCLUSIONS

Based on the full-scale load test performed on the 760 mm (30 inch) diameter ACIP with the reaction piles in layered sand the following conclusion are advanced:

1. The ACIP pile in the sand performed very well in terms of compressive load capacity and load-displacement relationship. The load-displacement relationship was modelled using the Vipulanandan ACIP pile model.
2. The skin frictions in compression have been quantified. The ACIP pile maximum measured skin friction in compression was correlated to the Texas Cone Penetrometer blow count. Also the ACIP piles the skin friction-displacement relationships in compression were modelled.

## ACKNOWLEDGEMENT

This study was supported by the Center for Innovative Grouting Materials and Technology (CIGMAT) with funding from the Texas Department of Transportation. The sponsor is not responsible for any of the conclusions made in this study.

## REFERENCES

- ASTM D 1143-07 (2013), "Testing Piles Under Static Compressive Load," *ASTM International*, West Conshohocken, PA.
- Brettmann, T. and NeSmith, W. (2005). "Advances in Auger Pressure Grouted Piles: Design, Construction and Testing," *Geotechnical Special Publication No. 132*, ASCE, pp. 12-14.
- Brown, D. (2005) "Axial Capacity of Augered Displacement Piles at Auburn University." ASCE, GSP 132.
- Davisson, MT (1972). "High Capacity Piles", *Proc., Lecture Series Innovations in Fndn. Construction*, ASCE Illinois Section, Chicago, 52 p.
- Deep Foundations Institute (DFI) (2016) *Augered Cast-in-Place Pile Manual*, Hawthorne, New Jersey
- McRae, J. B. and Simmonds, T. (1991). "Long-Term Stability of Vibrating Wire Instruments: One Manufacturer's Perspective," *Proc, The 3rd International Symposium on Field Measurements in Geomechanics*, Norway, pp. 283- 293.
- Neely, W. J. (1991). "Bearing Capacity of Auger-Cast Piles in Sand," *Journal of Geotech. Engrg.*, ASCE 117(2), 331-345.
- Texas Department of Transportation (TxDOT) (2012). *Geotechnical Manual* (<http://onlinemanual.txdot.gov>)
- O'Neill, M. W. (1994). "Review of Augered Pile Practice Outside the United States," *Transportation Research Record No. 1447*, TRB, Washington D. C, pp. 3-9.
- O'Neill, M. W., Vipulanandan, C., Ata, A., and Tan, F. (1999). "Axial Performance of Continuous Flight Auger Piles for Bearing," *Final Report*, TxDOT Project No. 7-3940, University of Houston, Houston, Texas.

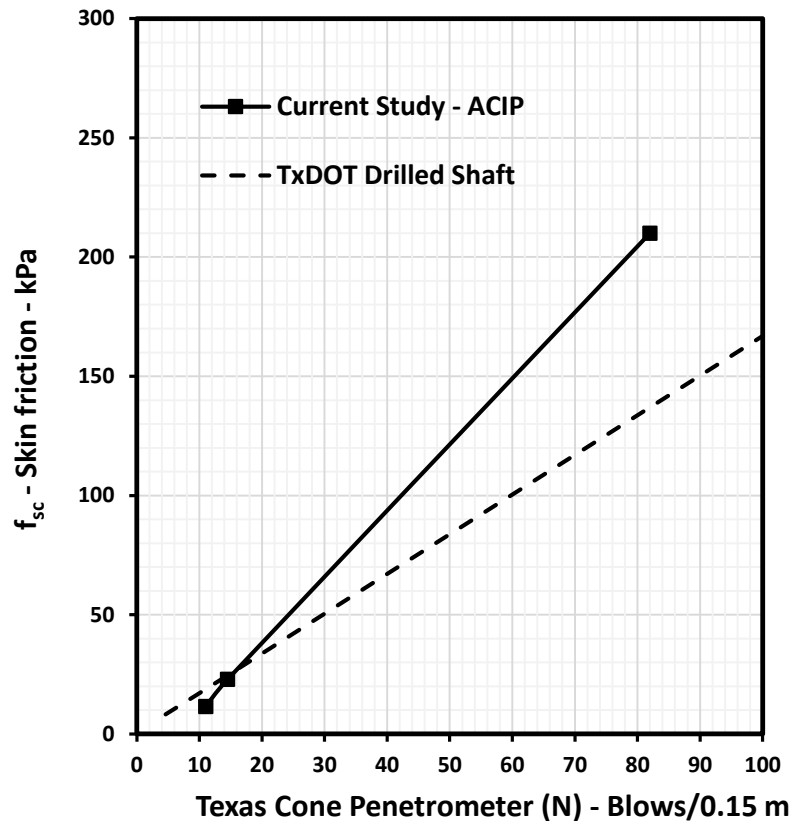


**Figure 7. TCP Correlation to Drilled Shaft and ACIP Pile in Sand.**

- Vigginai, C. (1989). "Influenza dei fattori tecnologici sul compartimento dei pali." *Atti. XVII Convegno Nazionale di Geotecnica. Taormina*, Vol. 2, pp. 83-91.
- Vipulanandan, C., and Paul, E. (1990). Performance of epoxy and polyester polymer concrete. *Materials Journal*, 87(3), 241-251.
- Vipulanandan, C. and Krishnan, S., (1993) "XRD Analysis and Leachability of Solidified Phenol-Cement Mixtures," *Cement and Concrete Research*, Vol. 23, pp. 792-802.
- Vipulanandan, C., Tand, K. E. and Kaulgud, S. (2005) "Axial Load-Displacement Relationship and CPT Correlation for ACIP Piles in Texas Gulf Coast Soils", *Proceedings, Advances in Designing and Testing Deep Foundations, GSP 129*, ASCE Geo Institute, pp. 290-308.
- Vipulanandan, C., Guvener, O. and McClelland M. (2007). "Monitoring and Curing of a Large Diameter ACIP Piles in Very Dense Sand," CD Proceedings (CD), GSP 158, Contemporary Issues in Deep Foundations, ASCE Geo Institute.
- Vipulanandan, C., Vembu, K. and Brettmann, T. (2009). "Load Displacement Behavior of ACIP Piles in Cohesive Soils." Proc. Contemporary Topics in Deep Foundations, ASCE GSP 185, 422-429.
- Vipulanandan, C., Vembu, K. and Guvener, O. (2012) 'Monitoring Auger Cast in Place Pile: Construction and Testing in Hard Clay.' *Proc. 37<sup>th</sup> Annual Conference on Deep Foundations*, Houston, Texas.

- Vipulanandan, C., and Mohammed, A. (2015). "Smart Cement Modified with Iron Oxide Nanoparticles to Enhance the Piezoresistive Behavior and Compressive Strength for Oil Well Applications". *Smart Materials and Structures*, 24(12).
- Vipulanandan, C., and Mohammed, A. (2016). "XRD and TGA, Swelling and Compacted Properties of Polymer Treated Sulfate Contaminated CL Soil," *ASTM Journal of Testing and Evaluation*, , Vol. 44, No. 6, pp. 2270-2284.